

Sulbha Sharma · Alok Dube · Biplab Bose
Pradeep K Gupta

Pharmacokinetics and phototoxicity of purpurin-18 in human colon carcinoma cells using liposomes as delivery vehicles

Received: 24 February 2005 / Accepted: 30 June 2005 / Published online: 2 August 2005
© Springer-Verlag 2005

Abstract Pharmacokinetics and phototoxicity of purpurin-18 (Pp18) in human colon carcinoma cells (Colo-205) was studied using liposomes as delivery vehicles. Cytotoxicity was measured using 3-(4,5-dimethylthiazol-2-yl)-2,5-diphenyltetrazolium bromide (MTT) assay and neutral red uptake assay, and mode of cell death was assessed by the study of cell morphology and nuclear staining with Hoechst 33342-propidium iodide. Pp18 solubilized in dimethyl sulfoxide saline solution was observed to aggregate (Q-band absorption 740 nm), resulting in very poor cellular uptake. Pp18 incorporated in liposome remained in monomeric form (Q-band absorption 695 nm), but due to the presence of an anhydride ring in the molecule it readily yielded another photosensitizer, chlorin p6 (Q-band absorption 662 nm). Measurements at various pH showed that Pp18 in liposome was stable at acidic pH (6.5). Incubation of cells with 6.0 μ M Pp18 in liposome at pH 6.5 showed a rapid cellular uptake. Spectrofluorometric measurements showed the presence of both Pp18 and chlorin p6, indicating conversion of some amount of Pp18 into chlorin p6 in the cells. Fluorescence microscopy revealed that the fluorescence was localized mainly in the cytoplasm, sparing the nucleus. Illumination of cells to white light after 4-h incubation with Pp18 liposome preparation was observed to lead to dose-dependent decrease in cell viability. At low irradiation time, cells displayed formation of plasma membrane blebs and micronuclei typical of apoptotic cell death. In contrast, at higher irradiation time, cell swelling and vacuolization in nucleus was observed, suggesting cell death due to necrosis. Irradiation with narrow bandwidth light showed that at low pH, the relative phototoxicity due to pp18 was higher than that due to chlorin p6. It is suggested that

the pH-dependent conversion of pp18 to chlorin p6 can be exploited to increase PDT selectivity.

Keywords Apoptosis · Drug delivery · Necrosis · Photodynamic therapy · Photosensitizers.

Introduction

Photodynamic therapy of cancer is based on selective localization of a photosensitizer in a tumor, followed by the generation of reactive oxygen species when the tumor area is exposed to visible light of appropriate wavelength. The tumor selectivity of a photosensitizer is believed to depend on its chemical character. It is generally accepted that tumor selectivity increases with the hydrophobic character of the photosensitizer [1]. The low solubility of hydrophobic photosensitizers in aqueous media, however, leads to its aggregation and thus hampers its systemic delivery. The aggregation of the photosensitizer also reduces its photosensitizing efficacy, because only monomeric species are photoactive. To overcome these problems, liposomes have been used as delivery systems in several studies [2]. For example, Damoiseau et al. [3] have reported an increase in photosensitizing efficiency of Bacteriochlorin by liposome-incorporation in WiDr cells. It has been shown that hypocrellin-A incorporated in egg phosphatidylcholine liposome maintains its monomeric state and gives rise to higher tumor uptake as compared to the photosensitizer in dimethyl sulfoxide-solubilized saline [4]. Similar results have been reported for different photosensitizers with different tumor models [5–7].

In the present study, we investigated the photodynamic efficacy of purpurin-18 (Pp18) after incorporating it in phosphatidylcholine liposome. Pp18 is a hydrophobic chlorophyll derivative with a strong absorption band in the red region (695 nm). However, due to the presence of an anhydride ring in the molecule it readily yields another photosensitizer,

S. Sharma · A. Dube (✉) · B. Bose · P. K. Gupta
Biomedical Applications Section, Centre for Advanced
Technology, Indore 452013, India
E-mail: okdube@cat.ernet.in
Tel.: +91-731-2488487
Fax: +91-731-2488430

chlorin p6, the Q-band absorption for which is at 662 nm. We studied this conversion at different pH and observed that Pp18 remains stable in liposome at pH 6.0–6.5. This liposome preparation was used to study cellular uptake and phototoxicity in colon carcinoma cells. The mode of cell death was evaluated by examining cell morphology and DNA fragmentation microscopically.

Materials and methods

Cell culture

Human colon (Colo-205) cells were purchased from the National Centre for Cell Sciences (NCCS), Pune, India. The cells were maintained in Rosewell Park Institute medium (RPMI) supplemented with 10% fetal bovine serum (FBS), antibiotics, and 2.2 g l^{-1} sodium bicarbonate. The cells were grown in monolayers at 37°C in a 5% CO_2 humidified incubator (Nuaire, USA).

RPMI media, phosphate-buffered saline (PBS), trypsin, nystatin, 3-(4,5-dimethylthiazol-2-yl)-2,5-diphenyltetrazolium bromide (MTT), and FBS were obtained from Himedia, Mumbai, India. Neutral Red was sourced from Loba Chemie, Mumbai, India. Sodium pyruvate, streptomycin, and phosphatidylcholine were obtained from Sigma, St. Louis, MO, USA.

Photosensitizer and liposome preparation

Pp18 was prepared from chlorophyll, following the method described by Hooper et al [8]. Small unilamellar liposomes were prepared by injecting a 50- μl ethanolic solution of phosphatidylcholine (25 mg ml^{-1}) containing Pp18 into 1.0 ml de-aerated solution of PBS (100 mM, pH 6.5). To check the stability of Pp18 at different pH (6.0–8.0), either phosphate buffer or Tris–HCl buffer was used. Liposome suspension was stored at 4°C until further use. For determining the concentration of Pp18 in liposome, a 10- μl liposome suspension was mixed in 1.0 ml acetone, centrifuged, and then the absorbance of the supernatant was read on a Cintra 20 spectrophotometer (GBC, Australia). Photosensitizer concentration was calculated from the molar extinction coefficient of Pp18 in acetone at 401 ($104,000 \text{ M}^{-1} \text{ cm}^{-1}$) and 695 nm ($41,800 \text{ M}^{-1} \text{ cm}^{-1}$) [8].

Cellular uptake of Pp18

Cells were incubated in darkness with $6.0 \text{ }\mu\text{M}$ Pp18 in liposome in a medium containing 10% FBS at pH 6.5. Subsequent to incubation, the culture medium containing the photosensitizer was removed and the cell monolayer was washed three times with cold PBS. Cells were harvested using 0.25% trypsin and resuspended in PBS. The pH of the trypsin solution

and of the PBS was kept at 6.5 to prevent hydrolysis of Pp18. The fluorescence spectrum of cell suspension was measured with a Fluorolog-2 spectrofluorometer (Spex, USA) using wavelength 407 nm for excitation.

Photodynamic treatment

Cells were inoculated at a concentration of $\sim 2 \times 10^4$ cells per well in a 96-well microplate. After overnight incubation, cells were incubated for 4 h in darkness with $6.0 \text{ }\mu\text{M}$ Pp18 liposome in a medium containing 10% FBS at pH 6.5. Subsequently, the medium containing Pp18 liposome was removed, the cell monolayer was washed with the medium without serum, and a fresh growth medium at pH 7.4 was added. Cells were then exposed to white light from two fluorescent tubes covered with a perspex sheet. The light intensity at the position of the cells was 10 W m^{-2} , as measured by a power meter model AN/2 (Ophir). The cells were exposed to white light for different time periods from 0 to 40 min.

Alternatively, the cells in a multiwell plate were irradiated with narrow bandwidth light at 670 nm ($\pm 5 \text{ nm}$) or 700 nm ($\pm 20 \text{ nm}$) to determine the phototoxicity due to chlorin p6 and Pp18, respectively. Irradiation was carried out using an LC-122A light source (Ci tek, USA) equipped with fiber optic probes. The power at the plate level was measured with a power meter (Ophir) and adjusted by varying the height of the fiber optic tip and of the appropriate filters. The fluence was kept nearly the same ($\sim 17 \text{ W m}^{-2}$) for both 670 and 700 nm lights and the cells were exposed to each radiation for 20 s.

MTT assay

Following irradiation, the media in all the wells were replaced with fresh growth medium at pH 7.4. After 24 h, MTT assay was performed to determine phototoxicity following the method described by Mosman [9]. Briefly, 100 μl of medium containing 10 μl MTT (5 mg ml^{-1}) was added to each well and the cells incubated with the mixture for 4 h. The culture medium was removed and the formazan crystals formed were dissolved using isopropanol containing 0.4 N hydrochloric acid. The optical density was measured at 570 and 690 nm using a Power Wave 340 microplate reader (Bio-tek Instruments Inc., USA). Each experiment included two controls, one in which cells were treated with dye but not exposed to light, and another where cells were exposed to light but not treated with dye. Phototoxicity was calculated as the percent decrease in MTT reduction with respect to a control sample, which received no Pp18 and no light.

Neutral Red uptake

To assess the photo-induced damage to lysosomes, uptake of neutral red (a lysosomal-specific probe) by cells was studied [10, 11]. Cells were plated in a 96-well mi-

croplate treated with photosensitizer and irradiated as described. Following irradiation, the growth medium was replaced with a medium containing neutral red ($50 \mu\text{g ml}^{-1}$) and the cells were incubated for 3 h in darkness. Subsequently, the cells were washed with PBS and the neutral red taken up by the cells was extracted using acidified ethanol. Uptake of neutral red was monitored using the microplate reader at 540 nm. Phototoxicity was calculated as the percent decrease in neutral red uptake with respect to a control sample, which received no Pp18 and no light.

Visualization of photosensitizer localization

Cells incubated with photosensitizer were visualized with a Zeiss Axiovert 135TV fluorescence microscope equipped with a 100 \times , NA 1.3 oil immersion lens and a filter cube (390–410 nm for excitation and beyond 590 nm for emission). The images were recorded with a digital camera DC 350F (Leica, Germany) and qFluoro standard software (Leica, Germany).

Morphological changes of cells and nuclei

A monolayer of the photodynamically treated cells and the control cells was visualized with an Axiovert 135TV inverted microscope (Zeiss) under phase contrast 100 X, NA 1.3 oil immersion lens, and images were recorded as described.

Morphological examination of apoptotic and necrotic cells was carried out as follows: the cells were trypsinized, suspended in PBS, and combined with floating cells that detached out in media due to photodynamic treatment. The cells were centrifuged and fixed in a methanol/acetic acid (3:1, v/v) mixture overnight. The cells were dropped onto microscope slides, dried, and stained with a mixture of $1 \mu\text{g ml}^{-1}$ each of Bis-benzimidazole Hoechst 33342 (HS) (Sigma) and propidium iodide (PI) (Sigma) in PBS. The slides were observed under a fluorescent microscope (Axiovert 135TV, Zeiss, Germany) using a fluorescent filter cube (excitation 340–380 nm, barrier filter 430 nm; excitation 530–560 nm, barrier filter 580 nm), and images were recorded. As opposed to PI, HS freely enters live cells and stains the nuclei of viable cells as well as of cells that have died by apoptosis or necrosis. Apoptotic cells can be distinguished from viable and necrotic cells on the basis of nuclear condensation and fragmentation, as well as by increased fluorescent intensity of nuclei stained with HS.

Statistics

All the experiments were done at least three times. The data in Figs. 3 and 7 represent mean and standard deviation value obtained from three independent experiments. The results of all other experiments were

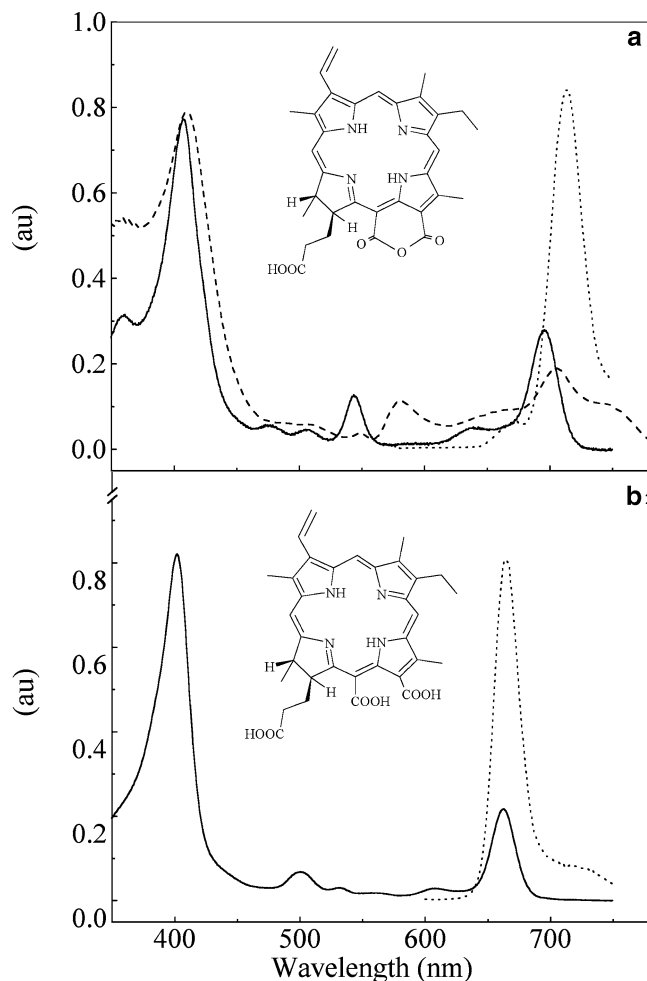


Fig. 1 **a** Absorption spectra of Pp18: *straight line*—in acetone, *dashed line*—solubilized in dimethyl sulfoxide and added to RPMI media containing 10% FBS, *dotted line*—405 nm excited fluorescence emission spectra in acetone. **b** Absorption spectra (*straight line*) and 401 nm excited fluorescence emission spectra (*dotted line*) of chlorin p6 in 0.1 N NaOH in 50% methanol. *Inset*: Chemical structure of the photosensitizers

qualitatively reproducible and, therefore, the result of a representative experiment is shown in figures.

Results and discussion

Chemical structure, absorbance spectra, and 405 nm excited fluorescence emission spectra of Pp18 and chlorin p6 are shown in Fig. 1. Pp18 is insoluble in aqueous media and aggregates when solubilized in dimethyl sulfoxide and added to RPMI media containing 10% FBS. The aggregated species showed broadening, a shift in q band absorbance to 740 nm (Fig. 1, dashed line), and loss of fluorescence. The fluorescence spectra of liposome preparation containing Pp18 at different pH are shown in Fig. 2a. At pH 7, chlorin p6 fluorescence at 668 nm dominated over fluorescence of Pp18 at 708 nm, indicating hydrolysis of Pp18. Lowering the medium pH was observed to reduce this conversion and at pH 6.0,

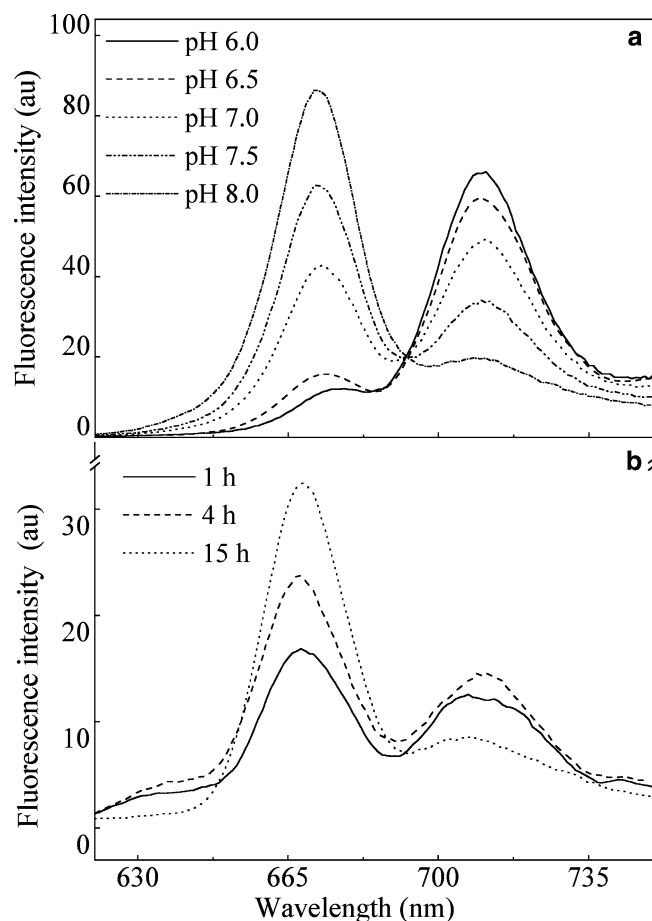


Fig. 2 Fluorescence emission spectra of Pp18. **a** Liposome suspension in Tris-HCl buffer at various pH. **b** Cell suspension in PBS at pH 6.5. Cells were incubated in darkness with 6.0 μ M Pp18 in liposome in growth media for various time periods, released by trypsinization, and suspended in PBS

fluorescence of only Pp18 was observed. Therefore, cellular uptake studies were carried out using Pp18 liposome preparation made in PBS at pH 6.5. The fluorescence spectra of cells at various time intervals following incubation with Pp18 liposome showed

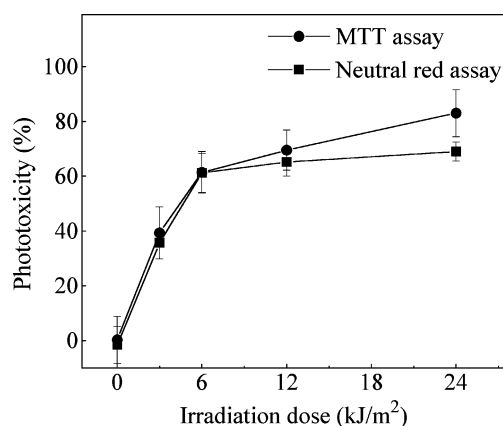
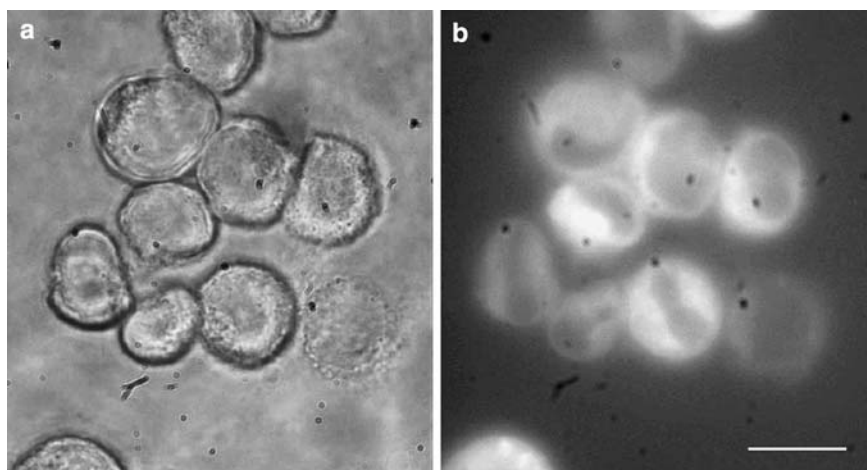


Fig. 3 Phototoxicity in Colo-205 cells following 4 h incubation with 6.0 μ M Pp18 in liposome and subsequent white light exposure at various irradiation doses. Circle—MTT assay, Square—Neutral red assay. Phototoxicity was calculated as percent decrease in MTT reduction or neutral red uptake with respect to a control sample, which received no Pp18 and no light. The zero dose point shows phototoxicity in cell sample incubated with Pp18 but not exposed to light

fluorescence due to both Pp18 and chlorin p6 (Fig. 2b). One hour after incubation with Pp18, the level of Pp18 and chlorin p6 was almost the same; later, at 4 h, both increased but the increase in 668 nm peak was larger compared to that for 708 nm. At a longer incubation time of > 15 h, the level of chlorin p6 increased further and a decrease was observed in the level of Pp18. These results show that Pp18 inside the cells get hydrolyzed slowly into chlorin p6.

Results of studies on cytotoxicity of Pp18 in Colo-205 cells following exposure to white light at different light doses are shown in Fig. 3. Percent phototoxicity was measured with respect to a control sample that received no drug and no light exposure. No toxicity was observed in cells treated with the drug but not exposed to light. Exposure to light was observed to lead to a dose-dependent decrease in viability. The viability curve showed a biphasic nature: an initial phase of rapid decline up to 6.0 kJ m⁻² followed by a slower phase.

Fig. 4 Microphotographs of Colo-205 cells following 4 h incubation with 6.0 μ M Pp18 in liposome in growth medium. **a** Phase contrast image. **b** Fluorescence image. Magnification 100 \times , bar—30 μ m



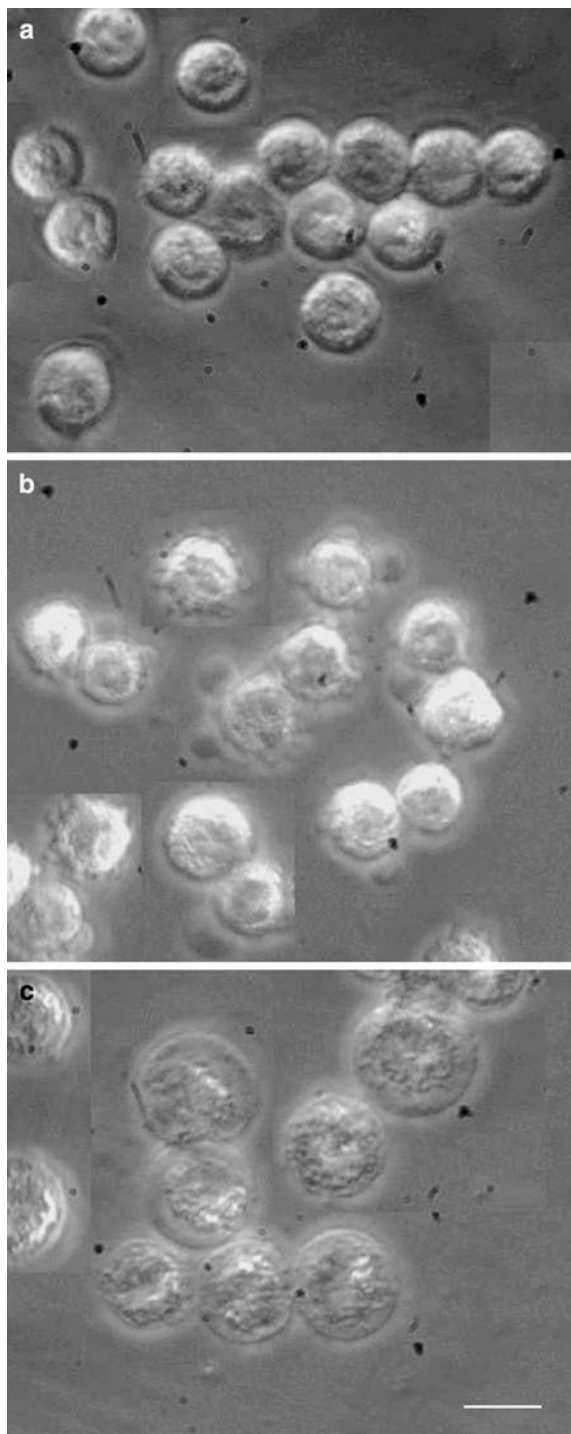


Fig. 5 Microphotographs of Colo-205 cells showing changes in cellular morphology following photodynamic treatment. Cells were incubated with $6.0 \mu\text{M}$ Pp18 in liposome for 4 h in growth medium. Phase contrast images at $100\times$ magnification for (a) cells kept in dark, (b) cells exposed to white light at 3.0 kJ m^{-2} and (c) 24 kJ m^{-2} , bar— $30 \mu\text{m}$

These results indicate saturation of damage at the target sites beyond 12 kJ m^{-2} . This trend was observed in both MTT assay and neutral red assay, which are measures of mitochondrial activity [12] and lysosomal

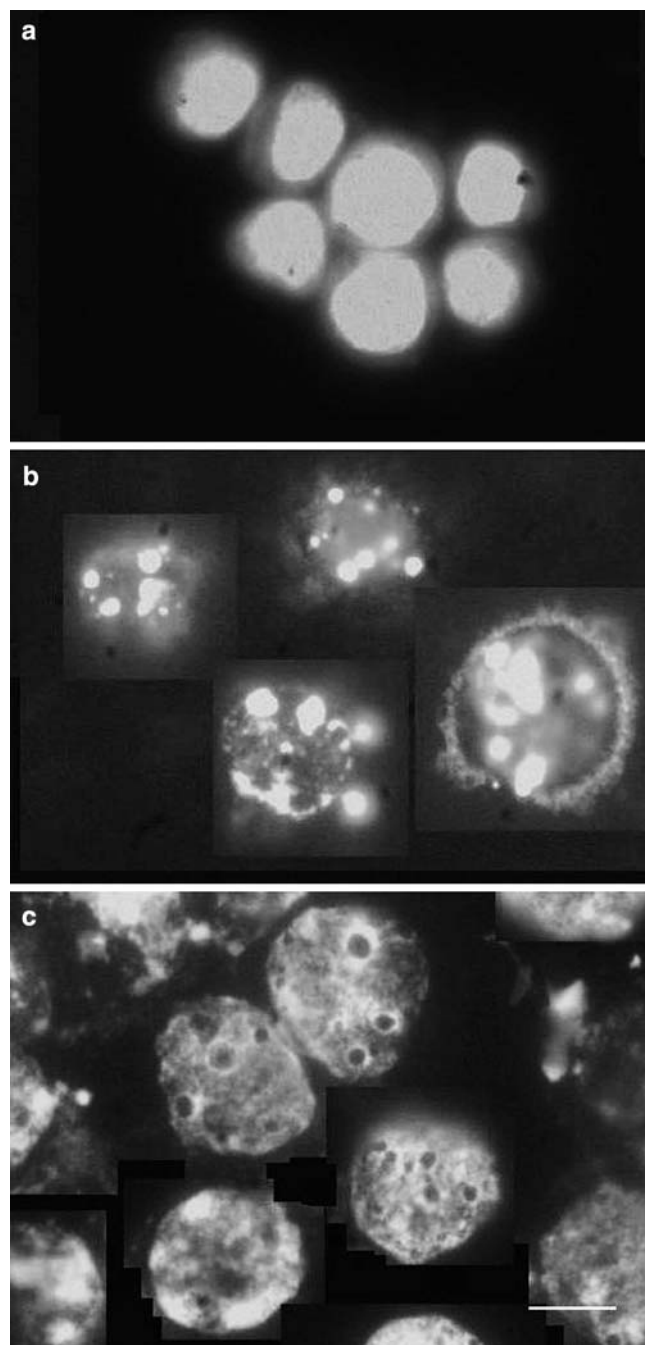


Fig. 6 Microphotographs of Colo-205 cells showing changes in nuclear morphology following photodynamic treatment and staining with HS and PI. Fluorescence images at $100\times$ magnification for (a) cells kept in dark, (b) cells exposed to white light at 3.0 kJ m^{-2} and (c) 24 kJ m^{-2} , bar— $30 \mu\text{m}$

activity, respectively [11]. The observed phototoxicity is because of the presence of both Pp18 and chlorin p6 in the cells. In our earlier studies on Colo-205 cells treated with aqueous solution of $10 \mu\text{M}$ chlorin p6 for 4 h in darkness, light exposure at 6 kJ m^{-2} was observed to damage only lysosomes but not mitochondria, and phototoxicity observed was $\sim 30\%$ of control [13]. In comparison, photodynamic treatment of Colo-205 cells

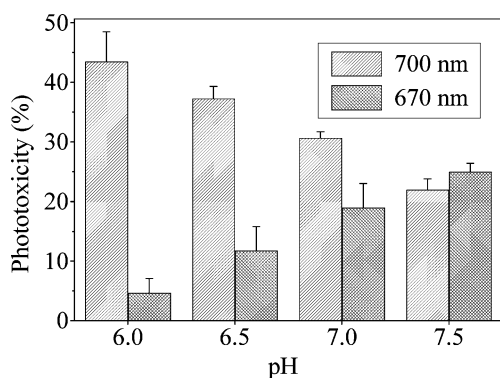


Fig. 7 Extracellular pH vs phototoxicity in Colo-205 cells following 1 h incubation with 6.0 μ M Pp18 in liposome and subsequent exposure to 670 or 700 nm light at 0.34 kJ m⁻². Phototoxicity was determined using MTT assay, and was calculated as percent decrease in MTT reduction with respect to a control sample that received no Pp18 and no light

at same the light dose under similar conditions but with 6.0 μ M Pp18 liposome preparation caused higher phototoxicity (60%), with significant damage to both mitochondria and lysosomes (Fig. 3). The increase in effectiveness of photodynamic treatment can be attributed to the presence of Pp18 together with chlorin p6 and efficient drug delivery of the photosensitizers in liposome preparation.

Mitochondria, endoplasmic reticulum, and lysosomes are the primary intracellular target sites responsible for inducing apoptotic cells death in PDT, whereas damage to plasma membrane is considered to be the cause of necrotic cell death [14]. The mode of cell death therefore depends on the site of photosensitizer localization in cells [14]. From the phase contrast and fluorescence images in Fig. 4, it is clear that the fluorescence of photosensitizers localized in the cytoplasmic region and spared the nucleus. In order to evaluate the mode of cell death, we studied the cellular morphology in the control cells and in the photodynamically treated cells. The cells treated with Pp18 liposome for 4 h in darkness show no sign of cell damage (Fig. 5a). Exposure to white light for 5 min was observed to lead to formation of plasma membrane blebs and shrinkage of cells (Fig. 5b). At higher irradiation time (40 min), an increase in cell size due to cell swelling was observed (Fig. 5c). Plasma membrane blebbing (zeiosis) is a well-defined characteristic of apoptotic cell death [15]. In contrast, cell swelling due to loss of plasma membrane integrity is a morphological change typical of necrotic cell death.

To further confirm these effects, we studied DNA fragmentation by fluorescence microscopy. The photomicrograph of cells stained with DNA-specific fluorescence probes HS-PI are shown in Fig. 6. The cells treated with Pp18 liposome for 4 h in darkness show the nucleus intact (Fig. 6a), whereas the cells exposed to white light for 5 min display chromatin condensation and formation of micronuclei or chromatin bodies indicative of apoptotic cell death (Fig. 6b). At higher irradiation time, necrotic cells with vacuolization of

nucleus are seen (Fig. 6c). These results together with the results on cell morphology presented in Fig. 5 suggest that photodynamic treatment with Pp18 liposome preparation leads to apoptosis at low irradiation dose and necrosis at higher irradiation dose. It is likely that a high dose of PDT resulted in inactivation of the elements of apoptosis and as a result necrosis ensued.

In Fig. 7 we show relative phototoxicity due to chlorin p6 and Pp18 in cells treated with pp18 liposome at different pH for 1 h. The phototoxic effect of 700 nm radiation was higher at a low pH than at physiological pH, whereas the opposite trend was observed for light of 670 nm. At low pH, phototoxicity due to 700 nm was greater as compared to phototoxicity due to 670 nm (Fig. 7). These results clearly show that low pH favored Pp18-mediated phototoxicity due to increase in stability of Pp18. Earlier, low pH has been shown to cause an increase in cellular uptake of the photosensitizers by increasing its hydrophobicity, and this was suggested to be a reason for the tumor-selective accumulation of some photosensitizers [13, 16, 17]. Although the increase in photosensitizer level would lead to higher tumor cell damage and increase in PDT selectivity, indirect tumor cell kill as a result of vascular shutdown has also been shown to contribute to the anti-tumor effect of PDT [18], and it is not known whether tumor vasculature might have a lower pH than normal vasculature.

To conclude, our results show that Pp18 can be stabilized in low pH liposomes and taken up efficiently by cells. The observed changes in cell morphology and nuclear material suggest that the mode of cell death depends on irradiation time. We propose that the pH-dependent conversion of Pp18 to chlorin p6 may be useful for photodynamic treatment of solid tumors where tissue pH is known to be slightly acidic. While Pp18 can remain relatively stable in the acidic environment of the tumor and would be retained in it due to its hydrophobic character, the higher physiological pH in normal tissue would favor its conversion into chlorin p6. We have recently shown that the binding of chlorin p6 to the lipid bilayer is less favored at pH > 6 due to its hydrophilic nature [19]. Therefore, it is less likely to be retained in normal tissues for longer periods of time. The pH difference in the tumor and in normal tissue is therefore expected to result in higher Pp18 concentration in the tumor at a certain time point after drug administration. Additionally, the difference in Q band absorption of Pp18 and chlorin p6 would allow selective destruction of tumor using narrow bandwidth light. This approach needs detailed in vivo investigations in an appropriate animal tumor model.

References

1. Ochsner M (1997) Photophysical and photobiological processes in photodynamic therapy of tumors. *J Photochem Photobiol B Biol* 39:1–18

2. Deryckel AS, de Witte PA (2004) Liposomes for photodynamic therapy. *Adv Drug Deliv Rev* 56:17–30
3. Damoiseau X, Schuitmaker HJ, Lagerberg JW, Hoebeke M (2001) Increase of the photosensitizing efficiency of the Bacteriochlorin a by liposome-incorporation. *J Photochem Photobiol B Biol* 60:50–60
4. Wang ZJ, He YY, Huang CG, Huang JS, Huang YC, An JY, Gu Y, Jiang LJ (1999) Pharmacokinetics, tissue distribution and photodynamic therapy efficacy of liposomal-delivered hypocrellin A, a potential photosensitizer for tumor therapy. *Photochem Photobiol* 70:773–780
5. Jiang F, Lilge L, Grenier J, Li Y, Wilson MD, Chopp M (1998) Photodynamic therapy of U87 glioma in nude rat using liposome-delivered Photofrin. *Lasers Surg Med* 22:74–80
6. Jiang F, Lilge L, Logie B, Li Y, Chopp M (1997) Photodynamic therapy of 9L gliosarcoma with liposome-delivered Photofrin. *Photochem Photobiol* 65:701–706
7. Lilge L, Wilson BC (1998) Photodynamic therapy of intracranial tissues: a preclinical comparative study of four different photosensitizers. *J Clin Laser Med Surg* 16:81–91
8. Hooper JK, Sery TW, Yamamoto N (1988) Photodynamic sensitizers from chlorophyll: purpurin-18 and chlorin p6. *Photochem Photobiol* 48:579–582
9. Mosman T (1983) Rapid colorimetric assay for cellular growth and survival application and cytotoxicity assays. *J Immunol Methods* 65:55–63
10. Lasarow RM, Issero RR, Gomez EC (1992) Quantitative in vitro assessment of phototoxicity by fibroblasts—Neutral Red assay. *J Invest Dermatol* 98:725–729
11. Sousa C, Sa e Melo T, Geze M, Gaullier JM, Maziere JC, Santos R (1996) Solvent polarity and pH effects on the spectroscopic properties of neutral red: application to lysosomal microenvironment probing in living cells. *Photochem Photobiol* 63:601–607
12. Musser DA, Osero AR (1994) The use of tetrazolium salts to determine sites of damage to the mitochondrial electron transport chain in intact cells following in vitro photodynamic therapy with photofrin II. *Photochem Photobiol* 59:621–626
13. Sharma M, Dube A, Bansal H, Gupta PK (2004) Effect of pH on uptake and photodynamic action of chlorin p6 on human colon and breast adenocarcinoma cell lines. *Photochem Photobiol Sci* 3:231–235
14. Plaetzer K, Kiesslich T, Verwanger T, Krammer B (2003) The modes of cell death induced by PDT: an overview. *Med Laser Appl* 18:7–19
15. Fadeel B (2004) Plasma membrane alterations during apoptosis: role in corpse clearance. *Antioxid Redox Signal* 6:269–275
16. Brault D (1990) Physical chemistry of porphyrins and their interactions with membranes: the importance of pH. *J Photochem Photobiol B* 6:79–86
17. Friberg EG, Cunderlikova B, Pettersen EO, Moan J (2003) pH effects on the cellular uptake of four photosensitizing drugs evaluated for use in photodynamic therapy of cancer. *Cancer Lett* 195:73–80
18. Krammer B (2001) Vascular effects of photodynamic therapy. *Anticancer Res* 21:4271–4277
19. Das K, Jain B, Dube A, Gupta PK (2005) pH dependent binding of chlorin-p6 with phosphatidyl choline liposomes. *Chem Phys Lett* 401:185–188